HNK-1 Glyco-epitope Regulates the Stability of the Glutamate Receptor Subunit GluR2 on the Neuronal Cell Surface*[s]

Ippei Morita[‡1], **Shinako Kakuda**[§1], **Yusuke Takeuchi**[§], **Satsuki Itoh**[¶], **Nana Kawasaki**[¶], **Yasuhiko Kizuka**[‡], **Toshisuke Kawasaki**[∥], and **Shogo Oka**[§2]

From the ‡Department of Biological Chemistry, Graduate School of Pharmaceutical Sciences, and §Department of Biological Chemistry, Human Health Sciences, Graduate School of Medicine, Kyoto University, Kyoto 606-8507, the ¶Division of Biological Chemistry and Biologicals, National Institute of Health Sciences, Tokyo 158-8501, and the ∥Research Center for Glycobiotechnology, Ritsumeikan University, Shiga 525-8577, Japan

HNK-1 (human natural killer-1) glyco-epitope, a sulfated glucuronic acid attached to *N*-acetyllactosamine on the nonreducing termini of glycans, is highly expressed in the nervous system. Our previous report showed that mice lacking a glucuronyltransferase (GlcAT-P), a key enzyme for biosynthesis of the HNK-1 epitope, showed reduced long term potentiation at hippocampal CA1 synapses. In this study, we identified an α-amino-3-hydroxy-5-methylisoxazole propionate (AMPA)-type glutamate receptor subunit, GluR2, which directly contributes to excitatory synaptic transmission and synaptic plasticity, as a novel HNK-1 carrier molecule. We demonstrated that the HNK-1 epitope is specifically expressed on the *N*-linked glycan(s) on GluR2 among the glutamate receptors tested, and the glycan structure, including HNK-1 on GluR2, was determined using liquid chromatography-tandem mass spectrometry. As for the function of HNK-1 on GluR2, we found that the GluR2 not carrying HNK-1 was dramatically endocytosed and expressed less on the cell surface compared with GluR2 carrying HNK-1 in both cultured hippocampal neurons and heterologous cells. These results suggest that HNK-1 stabilizes GluR2 on neuronal surface membranes and regulates the number of surface AMPA receptors. Moreover, we showed that the expression of the HNK-1 epitope enhanced the interaction between GluR2 and N-cadherin, which has important roles in AMPA receptor trafficking. Our findings suggest that the HNK-1 epitope on GluR2 regulates cell surface stability of GluR2 by modulating the interaction with N-cadherin.

HNK-1 glyco-epitope (HSO_3-3GlcAβ1–3Galβ1–4GlcNAc) is characteristically expressed on some cell adhesion molecules (NCAM, L1, and MAG, etc.) and extracellular matrix molecules (tenascin-R and phosphacan, etc.) in the nervous system (1). It has been reported that HNK-1 mediates the interaction of these adhesion molecules, thereby controlling their functions, including cell-to-cell adhesion (2), migration (3), and neurite extension (4). The unique structural feature of the HNK-1 epitope is the sulfated glucuronic acid, because sialic acids are usually attached to the terminal galactose residue of the inner *N*-acetyllactosamine structure (Galβ1–4GlcNAc) on various glycoproteins. HNK-1 is sequentially biosynthesized by one of two glucuronyltransferases (GlcAT-P or GlcAT-S)[3] (5, 6) and a sulfotransferase (HNK-1ST) (7). These enzymes are thought to localize and function in the Golgi apparatus, especially the trans-Golgi to trans-Golgi network, like most sialyltransferases and galactosyltransferases (8).

We previously demonstrated that mice deficient in GlcAT-P showed an almost complete loss of HNK-1 expression in the brain and exhibited reduced LTP in hippocampal CA1 synapses (9). Similarly, HNK-1ST-deficient mice also exhibited a reduction of LTP, and several other studies also revealed that HNK-1 is associated with neural plasticity (10–12). A recent study showed that β4-galactosyltransferase-2 synthesizes the glycan backbone structure of HNK-1, Galβ1–4GlcNAc. The mice lacking β4-galactosyltransferase-2 showed decreased HNK-1 expression in their brains and also exhibited impaired learning and memory (13). Overall, these studies suggest that HNK-1 plays unique functional roles in some types of neuronal plasticity, but the molecular mechanisms of HNK-1 remain unclear.

AMPA-type glutamate receptors mediate most of the fast excitatory synaptic transmissions in the mammalian brain and control synaptic strength. The regulated trafficking of AMPA receptors to the postsynaptic membrane is thought to be a major mechanism contributing to long lasting changes in synaptic strength, including LTP and long term depression (14, 15). AMPA receptors are mainly heterotetrameric channels assembled from the subunits GluR1 to GluR4, and all subunits have 4–6 potential *N*-glycosylation sites in their extracellular domains (16). Few studies have focused on the function of

[s] The on-line version of this article (available at http://www.jbc.org) contains supplemental Figs. S1 and S2.

[1] Both authors contributed equally to this work.
[2] To whom correspondence should be addressed: Kawahara-cho 53, Shogoin, Sakyo-ku, Kyoto 606-8507, Japan. Tel./Fax: 81-75-751-3959; E-mail: shogo@hs.med.kyoto-u.ac.jp.

[3] The abbreviations used are: GlcAT, glucuronyltransferase; AMPA, α-amino-3-hydroxy-5-methylisoxazole propionate; FT-ICR MS, Fourier transform-ion cyclotron resonance mass spectrometer; LC/MS/MS, liquid chromatography-tandem mass spectrometry; LTP, long term potentiation; PSD, postsynaptic density; CHO, Chinese hamster ovary; DTSSP, 3,3′-dithiobis(sulfosuccinimidyl propionate); P, postnatal day; ST, sulfotransferase.

N-glycosylation in AMPA receptors. Some investigations showed that AMPA receptor subunits expressed at both the cell surface and synaptic sites possess the mature glycosylated form (17, 18), but it is generally accepted that *N*-glycosylation is not essential for their channel function or ligand binding (19, 20).

In this study, we searched for a candidate molecule(s) responsible for the defects in synaptic plasticity seen in GlcAT-P-deficient mice. We found that the HNK-1 epitope is mainly expressed on a specific molecule in the hippocampal postsynaptic density (PSD) fraction. We focused on the molecule and identified a subunit of AMPA-type glutamate receptors, GluR2, as a novel HNK-1 carrier protein. Furthermore, we showed that the loss of HNK-1 epitope on GluR2 greatly increases both constitutive and regulated endocytosis of GluR2, resulting in a decrease in the amount of surface GluR2 in cultured hippocampal neurons and CHO cells. This is the first report demonstrating that the *N*-glycan on GluR2 regulates its protein function, and our results suggest that HNK-1 epitope on GluR2 is an important factor for synaptic plasticity.

EXPERIMENTAL PROCEDURES

Expression Plasmids—The following mammalian expression plasmids have been described. The 3.2-kb XhoI-XbaI GluR2 fragment derived from pKC24 (pBluescript)-GluR2, which was donated by Dr. M. Mishina (Tokyo University) (21), was cloned into pcDNA3.1/myc-HisB (Invitrogen) to yield the plasmid pcDNA3.1-GluR2. The pIRES-GlcAT-P-HNK-1ST and pEF-BOS-GlcAT-P plasmids were described previously (5, 22). The pcDNA3.1-N-cadherin was a generous gift from Dr. A. Kinoshita (Kyoto University) (23).

Biochemical Subcellular Fractionation—Biochemical subcellular fractionation was performed according to the method of a previous report (24) with minor modifications. The hippocampi of C57 BL/6 mice were homogenized with 15 strokes at 800 rpm in 9 volumes of ice-cold homogenizing buffer (10 mM Tris-HCl (pH 7.4), 0.32 M sucrose, 1 mM EDTA, and protease inhibitor mixture (Nacalai Tesque)), and the homogenate was centrifuged at $1,000 \times g$ for 20 min to remove nuclei and large debris. The supernatant fluid (S1, postnuclear fraction) was centrifuged at $10,000 \times g$ for 20 min to pellet a crude synaptosome fraction (P2). The supernatant above the P2 fraction was centrifuged at $125,000 \times g$ for 1 h, and the pellet was designated as the light membrane fraction (P3). The P2 fraction was lysed hypo-osmotically and centrifuged at $25,000 \times g$ for 30 min to obtain the synaptosomal membrane fraction (LP1). The LP1 fraction was then suspended in 0.5% Triton X-100 in homogenizing buffer for 15 min and centrifuged at $125,000 \times g$ for 1 h to obtain the PSD fraction. All biochemical experiments were carried out on ice or at 4 °C. The protein concentration of each fraction was measured with DC protein assay kit (Bio-Rad).

Purification and Identification of Glycoproteins Bearing HNK-1 Epitope—HNK-1 carrier glycoproteins from the P2 fraction of the hippocampi were partially purified with HNK-1 antibody-conjugated beads. The purified proteins were isolated by SDS-PAGE and stained with Coomassie Brilliant Blue. The ~100-kDa protein band was digested with trypsin, and the peptide fragments were identified by LC/MS/MS as reported previously (25). Proteins were identified by searching Swiss Protein Database (mouse) using the Mascot (Matrixscience) and TurboSequest search engines (Thermo Fisher Scientific).

SDS-PAGE, Immunoblot, and Immunoprecipitation Analysis—Proteins were separated by SDS-PAGE with the buffer system of Laemmli (26) and then transferred to a nitrocellulose membrane. After blocking with 5% nonfat dried milk in phosphate-buffered saline containing 0.1% Tween 20, the membrane was incubated with primary antibodies. Horseradish peroxidase-conjugated secondary antibodies and ECL (Pierce) were used for protein detection. For immunoprecipitation under denaturing conditions, the PSD fraction was solubilized with 1 volume of 10 mM Tris-HCl (pH 7.4) buffer containing 1% SDS and boiled for 5 min, and then 5 volumes of immunoprecipitation buffer (20 mM Tris-HCl (pH 7.4), 2% Triton X-100, and 300 mM NaCl) and 4 volumes of H_2O were added to the sample. For immunoprecipitation under native conditions, HEK 293 cells were lysed with extraction buffer (20 mM Tris-HCl (pH 7.4), 1% Triton X-100, 0.5% deoxycholate, 150 mM NaCl, 1 mM EDTA, and protease inhibitor mixture). Primary antibodies were used at 4 μg/ml, and 20 μl of protein G-Sepharose 4 Fast Flow (GE Healthcare) were added to precipitate the immunocomplexes for 2 h at 4 °C. The antibodies used in the immunoprecipitation and immunoblot analyses are listed as follows: HNK-1 monoclonal antibody (a hybridoma cell line was purchased from the American Type Culture Collection); anti-actin N terminus (Sigma); anti-PSD-95 (Chemicon); anti-GluR1 N terminus and anti-GluR2 N terminus (Zymed Laboratories Inc.); GluR2/3 (Upstate); anti-NR1 (Upstate); anti-NR2A (Upstate); anti-synaptophysin (FabGennix); and anti-N-cadherin (BD Biosciences).

N-Glycosidase F Digestion—The immunoprecipitates formed with the anti-GluR1 and anti-GluR2 antibodies were denatured with 20 mM sodium phosphate buffer (pH 7.2) containing 0.5% SDS, 1% 2-mercaptoethanol, and 4 mM EDTA. To reduce the concentration of SDS, we diluted the samples with 4 volumes of 20 mM sodium phosphate buffer (pH 7.2) containing 0.5% Nonidet P-40. Two units of *N*-glycosidase F (Roche Applied Science) were added to the solution, and the solution was incubated for 16 h at 37 °C.

Purification of GluR2—Anti-GluR2 antibody was raised from a rabbit immunized with a 20-mer peptide (QNFATYKEGYN-VYGIESVKI) corresponding to the C terminus of mouse GluR2 and purified with an antigen peptide affinity column. The purified anti-GluR2 antibody (3 mg) was coupled to 1.5 ml of CNBr-activated Sepharose 4B (GE healthcare), and the resin was packed into a column. The P2 fractions from 4-week-old mouse hippocampi were extracted with extraction buffer containing 1% *n*-dodecyl-β-D-maltopyranoside. The extracted material was slowly applied to the anti-GluR2 antibody column. After washing the column with Tris-buffered saline containing 0.1% *n*-dodecyl-β-D-maltopyranoside, GluR2 proteins bound to the resin were eluted with the elution buffer (50 mM diethylamine (pH 11.0), 150 mM NaCl, and 0.1% *n*-dodecyl-β-D-maltopyranoside). This eluate was immediately neutralized with 0.5 M NaH_2PO_4 (pH 4.5). The purified GluR2 was concentrated and subjected to SDS-PAGE.

LC/MS/MS of N-Linked Oligosaccharides—The bands of purified GluR2 (~100 kDa) were excised and cut into pieces. The gel pieces were destained and dehydrated with 50% acetonitrile. The protein in the gel was reduced and carboxymethylated by incubation with dithiothreitol and sodium monoiodoacetate (27). *N*-Glycans were extracted from the gel pieces as reported (28) and reduced with $NaBH_4$. The borohydride-reduced glycans were desalted with Envi-carb (Supelco). LC/MS/MS was carried out on a quadrupole linear ion trap/Fourier transform-ion cyclotron resonance mass spectrometer (FT-ICR MS) (Thermo Electron Corp) connected to a NanoLC system (Michrom BioResource, Inc.). The eluents were 5 mM ammonium acetate (pH 9.6), 2% CH_3CN (pump A), and 5 mM ammonium acetate (pH 9.6), 80% CH_3CN (pump B). The borohydride-reduced *N*-linked oligosaccharides were separated on a Hypercarb (0.1 × 150 mm, 5 μm; Thermo Electron Corp.) with a linear gradient of 5–20% of pump B (0–45 min), 20–50% of pump B (45–90 min), 50–70% of pump B (90–90.1 min), and 70% of pump B (90.1–130 min). A full MS scan (*m/z* 700–2000) by FT-ICR MS followed by data-dependent MS/MS for the most abundant ion was performed in the positive ion mode.

Cell Culture and Transfection—Primary hippocampal cultures were prepared from postnatal day 0 mouse brains. Hippocampi were trypsinized for 10 min at 37 °C. Dissociated neurons were plated on BD Biocoat Poly-D-lysine Cellware 4-well culture slide (BD Biosciences) at $1.0 × 10^5$ cells per well coated with 2 μg/ml laminin in Neurobasal medium (Invitrogen) supplemented with 2% B-27 (Invitrogen) and 500 μM L-glutamine. Every 7 days, the cultures were fed by replacing half of the medium with feeding medium. HEK 293 cells were cultured in Dulbecco's modified Eagle's medium with 10% fetal calf serum, and CHO cells were maintained in minimum Eagle's α-medium supplemented with 10% fetal calf serum. These cells were transfected using FuGENE 6 transfection reagent (Roche Applied Science).

Immunofluorescence-based Internalization Assays—Live hippocampal neurons were prelabeled with 10 μg/ml anti-GluR2 N terminus antibody for 15 min at 37 °C. After washing out the antibody, the neurons were incubated with or without 100 μM AMPA treatment (in the presence of 50 μM D-2-amino-5-phosphonopentanoic acid) for 20 min at 37 °C to allow endocytosis of GluR2. To stain GluR2 remaining on the cell surface, neurons were fixed in 4% paraformaldehyde, 4% sucrose for 10 min at room temperature and incubated with Alexa 488-conjugated secondary antibody (Molecular Probes) for 1 h at room temperature. The neurons were fixed with methanol at −20 °C, and Alexa 546-conjugated secondary antibody (Molecular Probes) was used for internalized GluR2 staining. Internalized and surface GluR2 fluorescence intensity was quantified using FluoView (Olympus) imaging system.

Cell Surface Protein Biotinylation Assay—Hippocampal cultured neurons and CHO cells were reacted with 1 mg/ml EZ-Link Sulfo-NHS-SS-biotin (Pierce) in phosphate-buffered saline for 30 min at 4 °C. Before surface biotinylation, neurons were incubated with or without 100 μM AMPA treatment for 20 min at 37 °C. These cells were lysed with extraction buffer, and cell surface-biotinylated proteins were pulled down with immobilized streptavidin (Pierce) and immunoblotted with anti-GluR2 antibody.

Cross-linking Experiment—Hippocampal P2 fractions and transfected HEK 293 cells were cross-linked with 2 mM 3,3′-dithiobis(sulfosuccinimidyl propionate) (DTSSP) (Pierce) in phosphate-buffered saline at room temperature for 30 min, and the reaction was quenched by the addition of 50 mM Tris-HCl (pH 7.4). The cross-linked P2 fractions were solubilized with extraction buffer and centrifuged at 125,000 × *g* for 1 h to separate into two distinct fractions (1% Triton X-100-soluble and -insoluble fractions). The Triton X-100-insoluble fraction was solubilized with 10 mM Tris-HCl (pH 7.4) buffer containing 1% SDS. Both insoluble and soluble fractions were subjected to immunoprecipitation analysis.

Quantification and Statistical Analysis of Immunoprecipitation Experiment—For the immunoblot analysis, a luminoimage analyzer LAS-3000 (Fuji Film) was used for the detection of protein bands. Densitometry of these bands was performed using image analysis software ImageGauge (Fuji Film). Calibration curves of protein bands for GluR2 and N-cadherin showed good linearity (r^2 = 0.97072 (N-cadherin) and 0.95566 (GluR2)). To quantify the strength of interaction between GluR2 and N-cadherin, the intensity of co-immunoprecipitated N-cadherin or GluR2 was normalized by immunoprecipitated GluR2 or N-cadherin, respectively. Results are shown as percent of value relative to the wild-type or control cells. The statistical analyses performed are listed in the individual figure legends, and values are expressed as the means ± S.E.

RESULTS

Expression of HNK-1 Glyco-epitope in the Mouse Hippocampus—To search for a novel HNK-1 carrier protein(s) responsible for synaptic plasticity, we first examined the expression of HNK-1 glyco-epitope in P2 (crude synaptosome) fractions obtained from mouse hippocampi at several developmental stages (Fig. 1*A*). The expression of HNK-1 was barely detected at embryonic day 16. After birth, it reached a peak at postnatal day 14 (P14), which coincided with the major postnatal synaptogenic period, and gradually decreased in adulthood. The expression of HNK-1 epitope was almost abolished in GlcAT-P-deficient mice (Fig. 1*A*), indicating that the biosynthesis of HNK-1 in brains is mainly regulated by a brain-specific glucuronyltransferase (GlcAT-P). Next, we performed biochemical fractionation of mouse hippocampi and examined the subcellular distribution of the HNK-1 epitope by immunoblot analysis. HNK-1 carrier proteins were detected in a wide range of molecular mass, from 100 to 250 kDa or higher (Fig. 1*B, upper panel*), and an ~100-kDa HNK-1-positive band was highly enriched in the P2 and PSD fractions, showing a similar distribution profile to the postsynaptic marker PSD-95 (Fig. 1*B, lower panel*). We also examined the subcellular localization of the HNK-1 epitope in cultured hippocampal neurons at 19 days *in vitro*. The immunoreactivity against the HNK-1 antibody was diffusely distributed on dendritic shafts and spine heads (supplemental Fig. 1). The punctate staining pattern for HNK-1 on the spines was co-localized with PSD-95 and apposed to the presynaptic marker synaptophysin. These results indicated the presence of HNK-1 carrier protein(s) at postsynaptic sites, and
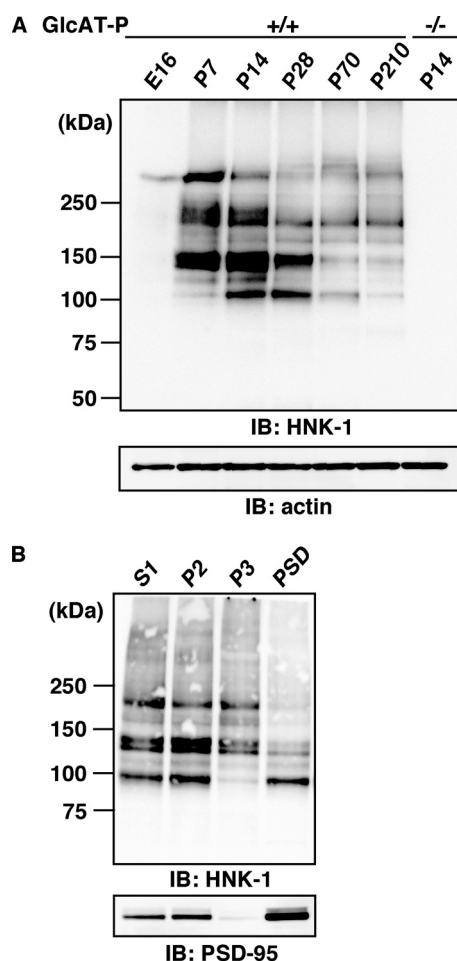
FIGURE 1. **HNK-1 is expressed in the PSD fraction from mouse hippocampi.** *A,* developmental expression of HNK-1 glyco-epitope in mouse hippocampi. Hippocampal P2 fractions (5 μg of proteins) obtained at the indicated developmental stages (*E16,* embryonic day 16; *P7* to *P210,* postnatal day 7–210) were immunoblotted (*IB*) with HNK-1 monoclonal antibody. Note that the expression of HNK-1 completely disappeared at P14 in the GlcAT-P$^{-/-}$ mice (*right lane*). *B,* biochemical fractionation of HNK-1 carrier proteins and PSD-95 in hippocampi. (*S1,* postnuclear supernatant; *P2,* crude synaptosome; *P3,* light membrane). Five micrograms of proteins obtained from different fractions were immunoblotted for HNK-1 and PSD-95.

we focused on the specific HNK-1 carrier molecule enriched at postsynaptic sites to examine the role of HNK-1 in synaptic plasticity.

HNK-1 Glyco-epitope Is Expressed on the AMPA-type Glutamate Receptor Subunit GluR2—To identify the ~100-kDa candidate glycoprotein, we purified HNK-1 carrier proteins from the P2 fractions of mouse hippocampi using HNK-1 antibody-conjugated beads. The purified proteins were isolated by SDS-PAGE and stained with Coomassie Brilliant Blue. A piece of polyacrylamide gel containing the ~100-kDa glycoprotein was excised and digested with trypsin. Using LC/MS/MS, we identified the novel HNK-1 carrier molecule as GluR2, which is an AMPA-type glutamate receptor subunit (supplemental Fig. 2). To further confirm these results, we immunoprecipitated GluR1 and GluR2 by subunit-specific antibodies from the PSD fractions of hippocampi under denaturing conditions and then immunoblotted them with HNK-1 antibody (Fig. 2*A*). HNK-1 epitope was specifically detected on GluR2 but not on GluR1. Furthermore, the HNK-1 epitope on GluR2 was completely
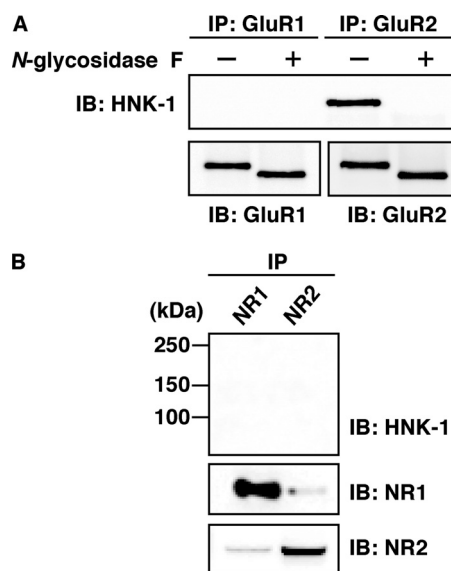

FIGURE 2. **Immunoprecipitation analysis of the PSD fractions from mouse hippocampi.** *A,* GluR1 and GluR2 were immunoprecipitated (*IP*) with GluR1- and GluR2-specific antibodies under SDS-denaturing conditions, respectively. The immunoprecipitates were treated with (+) or without (−) *N*-glycosidase F and then immunoblotted (*IB*) for HNK-1 (*upper panel*) and GluR1 or GluR2 (*lower panel*). *B,* NR1 and NR2 were immunoprecipitated and immunoblotted with HNK-1 antibody (*upper panel*), NR1 (*middle panel*), and NR2 (*lower panel*).

removed by *N*-glycosidase F treatment, indicating that it is attached to the nonreducing terminus of *N*-glycan(s) on GluR2. We also examined the expression of HNK-1 on *N*-methyl-D-aspartic acid (NMDA) receptor (composed of NR1 and NR2 subunits), which is another ionotropic glutamate receptor (Fig. 2*B*). Neither NR1 nor NR2 carried the HNK-1 epitope. These results suggest that the HNK-1 epitope is specifically expressed on GluR2 and may regulate the function of GluR2.

LC/MS/MS of N-Linked Oligosaccharides on GluR2—To determine the glycan structure, including HNK-1 glyco-epitope on GluR2, GluR2 was immunopurified from P2 fractions and separated by SDS-PAGE (Fig. 3*A*). The GluR2 band (~100 kDa) was excised and treated with *N*-glycosidase F. The extracted *N*-linked oligosaccharides were reduced with NaBH$_4$ and subjected to LC/MS/MS. Fig. 3*B* shows the base peak chromatograms obtained by a full MS scan (*m/z* 700–2000) by FT-ICR MS. The major molecular ions detected by a full MS scan were subjected to data-dependent collision-induced dissociation-tandem mass spectrometry automatically. From all the MS/MS spectra, only those of oligosaccharides carrying HNK-1 or nonsulfated HNK-1 motifs were sorted out using HNK-1 diagnostic ion, GlcA-Gal-GlcNAc$^+$ (*m/z* 542) (Fig. 3*B, lower panel*). The carbohydrate structure of the HNK-1 and nonsulfated HNK-1 oligosaccharides (peaks 1–6) was deduced from the *m/z* values of precursor ions detected by FT-ICR MS and product ions obtained by MS/MS (Fig. 3*C*). As a typical MS/MS spectrum, the product ion spectrum of peak 3 is shown in Fig. 3*D*. Peak 3 was assigned to a bisected biantennary *N*-glycan carrying the HNK-1 motif based on the product ions, such as GlcA-Gal-GlcNAc$^+$ (*m/z* 542), SO$_3$-GlcA-Gal-GlcNAc$^+$ (*m/z* 622), and [M-SO$_3$-GlcA-Gal-GlcNAc + H]$^+$ (*m/z* 1319). Together with the immunoprecipitation experiment shown in

A

(kDa)
150 —
100 —
75 —

CBB   IB: GluR2   IB: HNK-1

B

Base peak chromatogram
MS (m/z 700–2000)

EIC
MS/MS (m/z 542)

3
970.822

4
1043.850

6
1095.855

5
869.280

1
930.846

2
1003.875

Relative Abundance

Time (min)

C

1

GlcA-Gal-GlcNAc-Man
　　　　　　　　　　GlcNAc-Man-GlcNAc-GlcNAc-OH
GlcNAc-Man
　　　　　　　　　1859.665

2

SO3-GlcA-Gal-GlcNAc-Man　　　　　Fuc
　　　　　　　　　　GlcNAc-Man-GlcNAc-GlcNAc-OH
GlcNAc-Man
　　　　　　　　　2005.724

3

SO3-GlcA-Gal-GlcNAc-Man
　　　　　　　　　　GlcNAc-Man-GlcNAc-GlcNAc-OH
GlcNAc-Man
　　　　　　　　　1939.623

4

SO3-GlcA-Gal-GlcNAc-Man　　　　　Fuc
　　　　　　　　　　GlcNAc-Man-GlcNAc-GlcNAc-OH
GlcNAc-Man
　　　　　　　　　2085.681

5

SO3-GlcA-Gal-GlcNAc-Man
　　　　　　　　　Man-GlcNAc-GlcNAc-OH
GlcNAc-Man
　　　　　　　1736.544

6

SO3-GlcA-Gal-GlcNAc-Man　　　　Fuc
　　　　　　　　Man-GlcNAc-GlcNAc-OH
GlcNAc-Man
NeuAc
　　　　　　　2189.692

D

GlcA-Gal-GlcNAc$^+$
542.4

SO3-GlcA-Gal-GlcNAc$^+$
622.2

[M-SO$_3$+ 2H]$^{2+}$
931.2

1116.6

1319.5

-GlcNAc　-GlcNAc　-SO$_3$-GlcA-Gal-GlcNAc

-Hex

-SO$_3$　-GlcNAc

1737.6

1657.5

1399.6
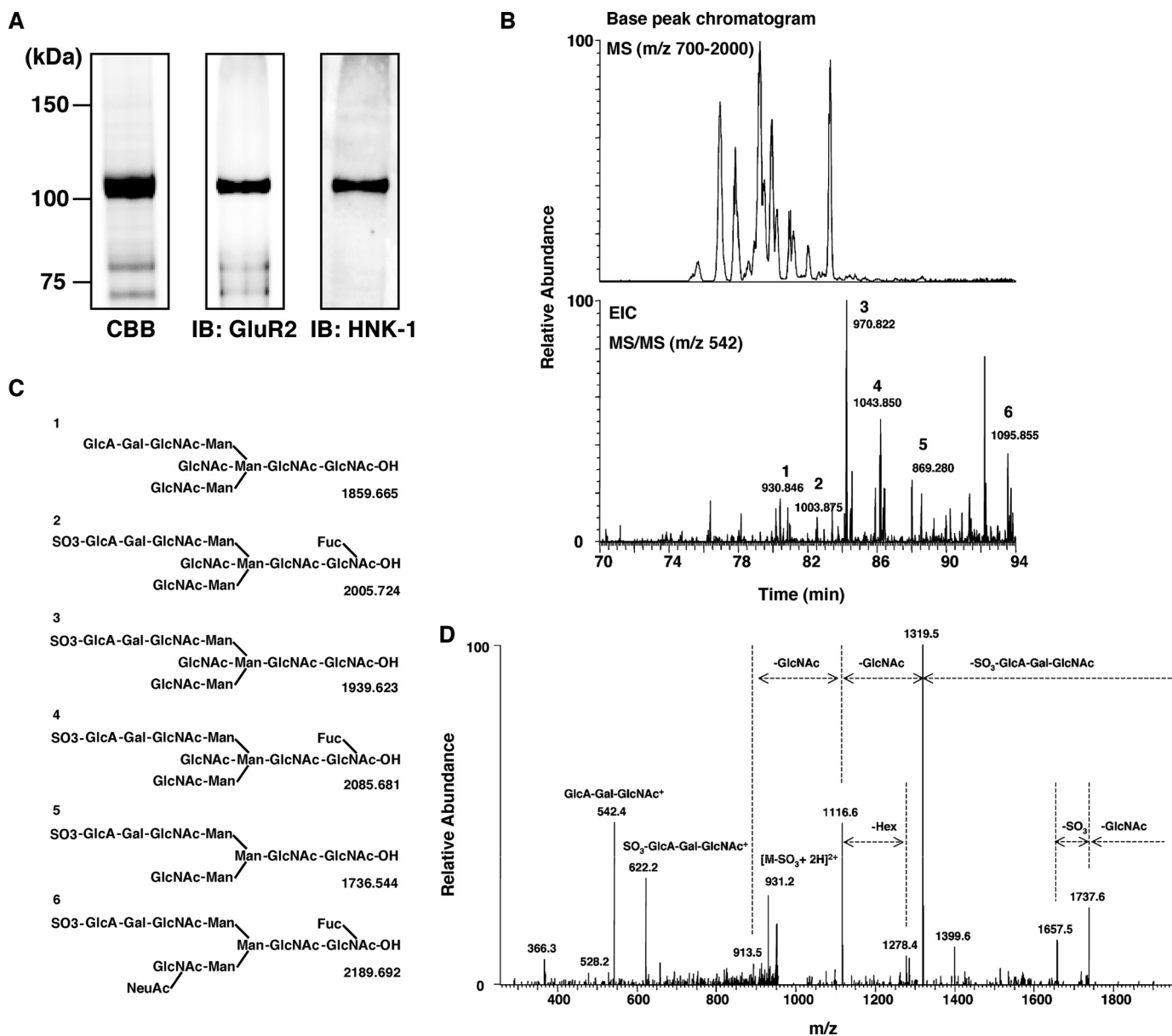
1278.4

913.5

528.2

366.3

Relative Abundance

m/z

FIGURE 3. **LC/MS/MS of *N*-linked oligosaccharides on GluR2.** *A,* GluR2 from the P2 fraction of hippocampi was purified using an anti-GluR2 antibody column. The purified GluR2 was digested with *N*-glycosidase F, and the extracted *N*-linked oligosaccharides were analyzed by LC/MS/MS. *B,* peak chromatogram obtained by a full MS scan (*m/z* 700–2000) of borohydride-reduced *N*-linked oligosaccharides released from the gel-separated GluR2 (*upper panel*). Extracted ion chromatogram (*m/z* 542) was from a data-dependent MS/MS scan, and *m/z* values of precursor ions were obtained by FT-ICR MS (*lower panel*). *C,* deduced structures of *peaks 1–6* and their theoretical masses as shown in *B*. *D,* MS/MS spectrum of peak 3 as shown in *B*.

Fig. 2, these data show that HNK-1 is actually expressed on *N*-glycans of GluR2 in the brain.

HNK-1 Glyco-epitope on GluR2 Regulates the Endocytosis of GluR2 in Hippocampal Neurons—Numerous recent studies have strongly suggested that the mechanism underlying activity-dependent synaptic plasticity is related to the redistribution of GluR2 between intracellular components and the synaptic membrane (15). GluR2 is internalized by clathrin-dependent endocytosis, and two distinct types of GluR2 endocytosis are known, constitutive (under basal conditions) and regulated endocytosis (under stimulation by a reagent such as AMPA, *N*-methyl-D-aspartic acid, and insulin) (29). Moreover, we revealed that HNK-1 is specifically expressed on GluR2 (Fig. 2) and that loss of HNK-1 in the brain impairs the synaptic plas-

ticity (8). Taken together, we hypothesized that HNK-1 expression on GluR2 regulates its intracellular distribution. To evaluate the influence of HNK-1 epitope on GluR2 endocytosis, we performed a fluorescence-based internalization assay (30) using hippocampal neurons derived from wild-type or GlcAT-P-deficient mice. In this assay, the surface GluR2 subunits on living neurons at 18 days *in vitro* were labeled with 10 μg/ml antibody against the extracellular epitope of GluR2, and then antibody-labeled neurons were incubated for 20 min at 37 °C to allow endocytosis either in the absence or presence of 100 μM AMPA to determine constitutive or regulated GluR2 endocytosis, respectively. The antibody-labeled GluR2 remaining on the cell surface and the GluR2 internalized into intracellular vesicles were independently immunostained under nonperme-
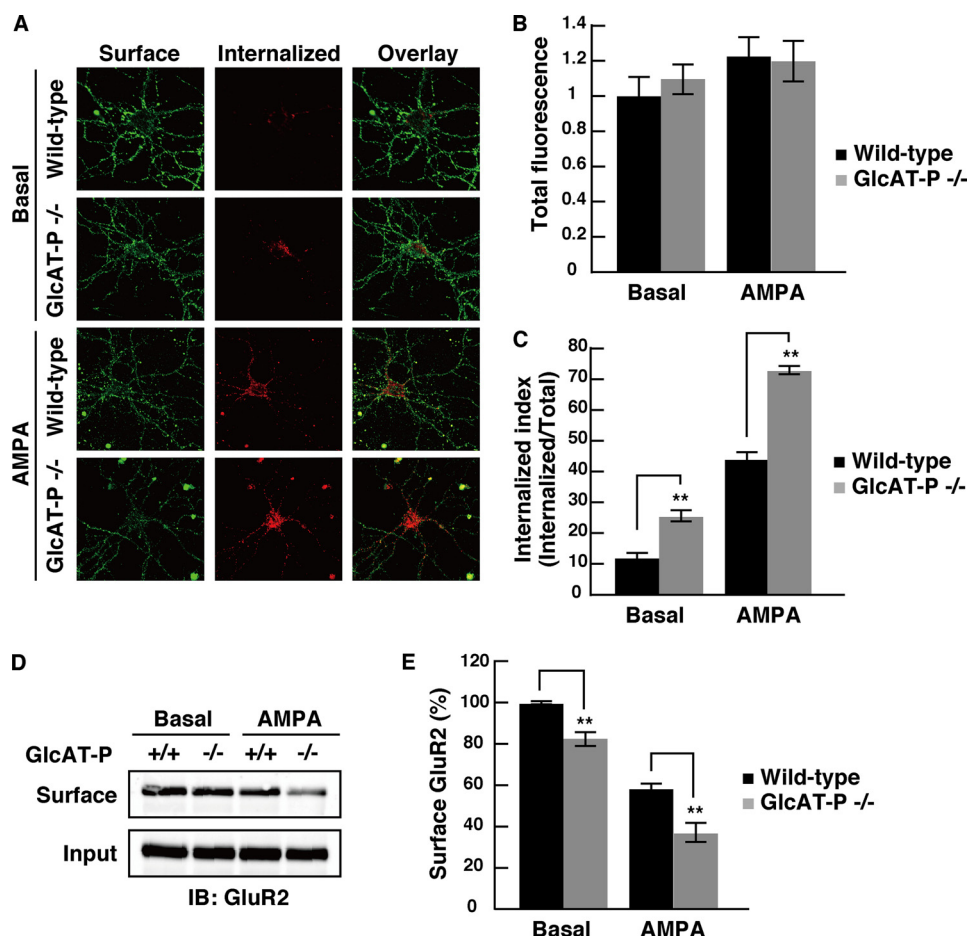
FIGURE 4. **Intracellular and surface GluR2 under basal and AMPA-stimulated conditions in cultured hippocampal neurons.** *A,* representative images of neurons stained for surface and internalized GluR2, following 20 min of incubation in conditioned medium or incubation in conditioned medium containing 100 μM AMPA plus 50 μM D-2-amino-5-phosphonopentanoic acid. *B,* quantification of total GluR2 fluorescence (surface + internalized GluR2) normalized to the value of GluR2 in wild-type neurons under the basal conditions (*n* = 17–26 for each condition). *C,* quantification of intracellular accumulation of GluR2, measured as the ratio of internalized fluorescence/total fluorescence (internalization index). **, *p* < 0.01 (two-tailed *t* test). *D,* biotinylation assay of surface GluR2. Under basal or AMPA-stimulated conditions, the cell surface proteins on hippocampal neurons were biotinylated, and biotinylated GluR2 was precipitated with streptavidin beads and immunoblotted (*IB*) with anti-GluR2 antibody. *E,* quantification of surface GluR2. The amount of surface GluR2 as shown in *D* was measured by band intensity and normalized to inputs, respectively (*n* = 3). **, *p* < 0.01 (two-tailed *t* test). *Error bars* indicate S.E.

abilizing and permeabilizing conditions, respectively (Fig. 4*A*). The total fluorescence (surface and internalized fluorescence) of all four conditions was unchanged (Fig. 4*B*). The "internalization index" represents the ratio of internalized fluorescence/total fluorescence and was compared with wild-type neurons under basal and AMPA-stimulated conditions (Fig. 4*C*). Under basal conditions, GluR2 in GlcAT-P-deficient neurons showed a higher degree of intracellular accumulation than GluR2 in wild-type neurons (wild-type, 11.7 ± 1.35; GlcAT-P$^{-/-}$, 25.1 ± 1.87; **, *p* < 0.01) (Fig. 4, *A* and *C*). Under AMPA-stimulated conditions, the amount of intracellular GluR2 in GlcAT-P-deficient neurons was more greatly increased than that in wild-type neurons (wild type, 43.7 ± 2.09; GlcAT-P$^{-/-}$, 72.5 ± 1.49; **, *p* < 0.01). Next we performed a cell surface biotinylation assay to test the surface levels of GluR2 in cultured hippocampal neurons. The amount of surface GluR2 in GlcAT-P-deficient neurons was slightly decreased to 82.5 ± 3.5% of wild type under the basal conditions (**, *p* < 0.01) (Fig. 4, *D* and *E*). After

AMPA treatment, the surface expression levels of GluR2 both in wild-type and GlcAT-P-deficient neurons were decreased, but the surface expression in GlcAT-P-deficient neurons was decreased more than that in wild type (wild type, 58.1 ± 2.6%; GlcAT-P$^{-/-}$, 35.5 ± 4.5; **, *p* < 0.01). These results from two independent experiments were consistent with each other and revealed that GluR2 in GlcAT-P-deficient neurons showed facilitated endocytosis or instability on the cell surface under both basal and stimulated conditions.

HNK-1 Epitope Is Involved in the Interaction between GluR2 and N-cadherin—A recent report has shown that the extracellular N-terminal domain of GluR2 interacts with N-cadherin and that the interaction plays important roles in the surface diffusion of GluR2 on neuronal membranes (31). It was also reported that the association between GluRs and N-cadherin regulates the trafficking and surface expression of AMPA receptors (32). As described above, it seems that HNK-1 deficiency leads to destabilization of GluR2 on the neuronal cell surface. To determine whether the HNK-1 epitope on the N-terminal domain is involved in the interaction of GluR2 with N-cadherin, we compared the amount of N-cadherin associated with GluR2 between the wild-type and GlcAT-P-deficient mice by means of a co-immunoprecipitation experiment. In brief, the P2 fraction prepared from hippocampi was treated with DTSSP for protein cross-linking and then solubilized with 1% Triton X-100. The GluR2-containing complex was immunoprecipitated from the Triton X-100-soluble and -insoluble fractions using anti-GluR2 antibody, and the cross-linking was then reversed and analyzed by immunoblot analysis with antibodies against GluR2 and N-cadherin, respectively. Because of the existence of synaptophysin and PSD-95 (Fig. 5*A, input, middle* and *lower panels*), we refer to the soluble and insoluble fractions as the pre- and postsynaptic protein-rich fractions, respectively. In the presynaptic protein-rich fraction (soluble fraction), the interaction between GluR2 and N-cadherin was hardly detected (Fig. 5*A*). GluR2 interacted with N-cadherin in the postsynaptic protein-rich fraction (insoluble fraction) from wild-type and GlcAT-P-deficient mice (Fig. 5*A*). However, the amount of N-cadherin co-immunoprecipitated with GluR2 in GlcAT-P-deficient mice significantly decreased to 64.8 ± 6.4% that in wild-type mice
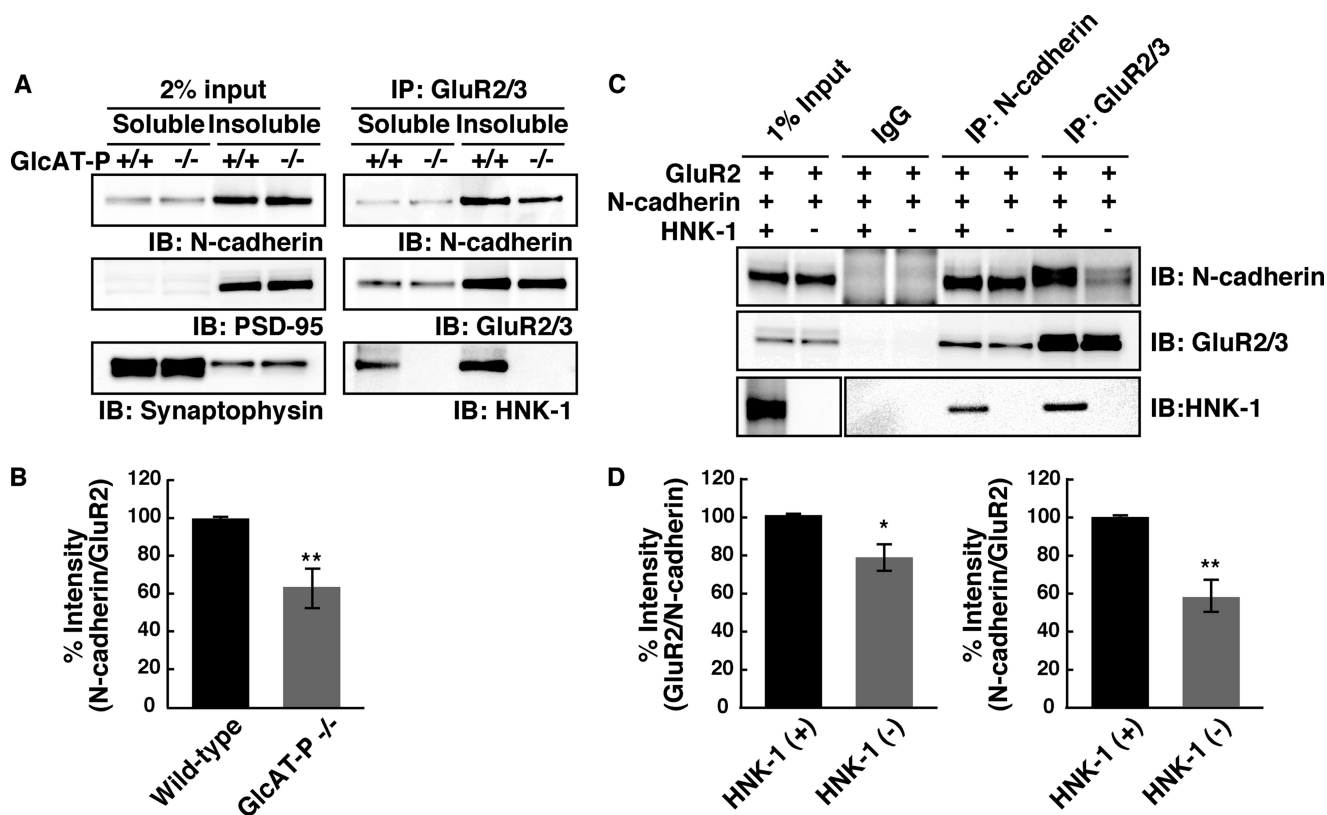
FIGURE 5. **HNK-1 glyco-epitope on GluR2 enhances the interaction with N-cadherin.** *A,* P2 fractions from hippocampi of wild-type and GlcAT-P$^{-/-}$ mice at P14 were cross-linked with DTSSP and then solubilized with 1% Triton X-100. Both soluble and insoluble fractions were immunoprecipitated (*IP*) with anti-GluR2/3 antibodies, and the immunoprecipitate complexes were immunoblotted (*IB*) for GluR2/3, N-cadherin, and HNK-1. Note that the fractions that contain synaptophysin or PSD-95 are the pre- and postsynaptic protein-rich fractions, respectively. *B,* quantification of N-cadherin co-immunoprecipitated with GluR2 in *A*. N-cadherin associated with GluR2 was normalized to immunoprecipitated GluR2 ($n = 5$). **, $p < 0.01$ (two-tailed *t* test). *C,* immunoprecipitation analysis of GluR2 interacting with N-cadherin in HEK 293 cells. HEK 293 cells were overexpressed with GluR2 and N-cadherin in the presence or absence of HNK-1-synthesizing enzymes (GlcAT-P and HNK-1ST), as indicated. After cross-linking with DTSSP, GluR2/3 or N-cadherin was immunoprecipitated. *D,* quantification of GluR2 associated with N-cadherin (*left panel*) and N-cadherin associated with GluR2 (*right panel*) in *C*. The results were normalized by immunoprecipitated N-cadherin ($n = 3$). *, $p < 0.05$; **, $p < 0.01$ (two-tailed *t* test). *Error bars* indicate S.E.

(Fig. 5*B*, **, $p < 0.01$), although the amounts of total N-cadherin and immunoprecipitated GluR2 exhibited no difference between wild-type and GlcAT-P-deficient mice. This result indicates that HNK-1 epitope enhances the interaction between GluR2 and N-cadherin at the postsynaptic membranes. To further corroborate this, N-cadherin and GluR2 expression plasmids were co-transfected into HEK 293 cells in the presence or absence of a plasmid containing HNK-1-synthesizing enzymes (GlcAT-P and HNK-1ST) for the production of GluR2 with or without the HNK-1 epitope. In both HNK-1-positive and -negative cells, the GluR2-N-cadherin interaction was detected (Fig. 5*C*). In the HNK-1-negative cells, the amount of N-cadherin co-immunoprecipitated with GluR2 decreased to $58.3 \pm 8.4\%$ (**, $p < 0.01$) that in the HNK-1-positive cells (Fig. 5, *C* and *D*), and in a reverse experiment, the amount of GluR2 co-immunoprecipitated with N-cadherin was reduced to $78.4 \pm 6.9\%$ (*, $p < 0.05$) that in the HNK-1-positive cells (Fig. 5, *C* and *D*). These results indicate that HNK-1 epitope enhances the physical interaction of GluR2 with N-cadherin.

HNK-1 Glyco-epitope Enhances the Surface Expression of GluR2 in an N-cadherin-dependent and -independent Manner—To corroborate that the interaction between GluR2 and N-cadherin modulated by HNK-1 epitope has an effect on the surface

expression of GluR2, we transiently expressed GluR2 and N-cadherin into CHO cells and performed a cell surface biotinylation assay. Unlike HEK 293 cells, CHO cells did not express endogenous N-cadherin. Co-expression of N-cadherin slightly increased the surface expression of GluR2 ($119.1 \pm 8.7\%$) (Fig. 6, *A* and *B*). To examine the effect of HNK-1 on the surface expression of GluR2, we next expressed the HNK-1 epitope on GluR2 by GlcAT-P and HNK-1ST in the absence or presence of N-cadherin. The expression of HNK-1 increased the surface level of GluR2 even in the absence of N-cadherin ($137.4 \pm 10.1\%$), but the effect of the HNK-1 was more obvious in the presence of N-cadherin ($238.2 \pm 34.5\%$). Taken together, these results indicated that the surface stability of GluR2 was enhanced by HNK-1 in both an N-cadherin-dependent and -independent manner.

DISCUSSION

In the nervous system, various types of cells recognize and interact with each other to form a precise neural network. During this process, carbohydrates expressed on proteins, especially cell surface and secreted proteins, give rise to the structural and functional diversities of carrier proteins. Among them, HNK-1 glyco-epitope is mainly expressed on immunoglobulin family cell adhesion molecules (NCAM, L1, P0, etc.)
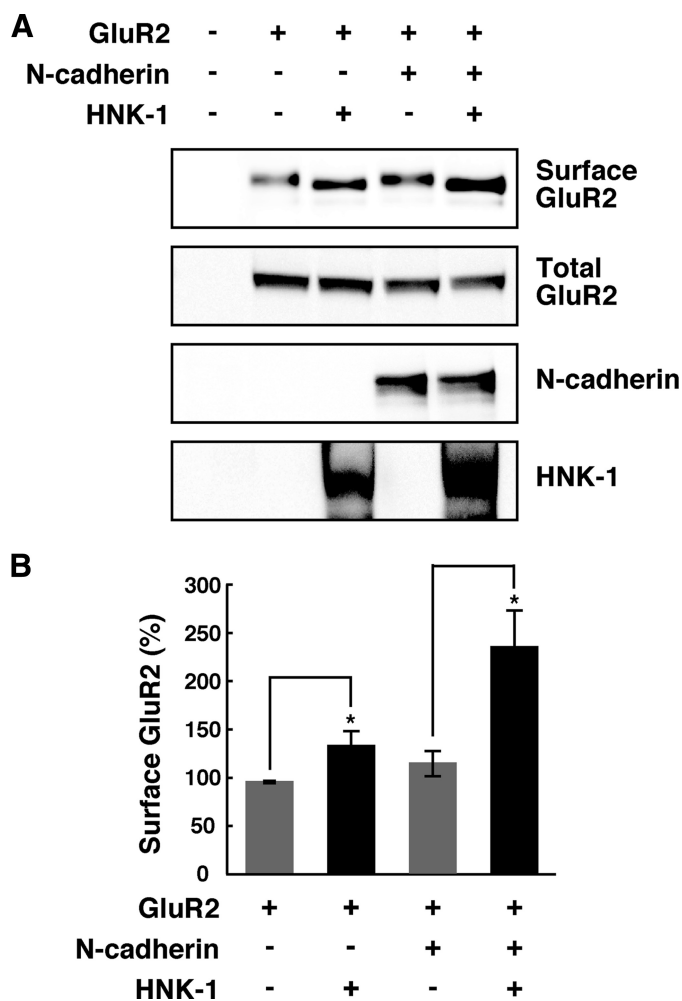
FIGURE 6. **HNK-1 glyco-epitope enhances the surface expression of GluR2 in an N-cadherin-dependent and -independent manner.** *A,* CHO cells were overexpressed with GluR2, N-cadherin, and HNK-1-synthesizing enzymes as indicated. The cell surface proteins on CHO cells were biotinylated, and biotinylated GluR2 molecules were precipitated with streptavidin beads and immunoblotted with anti-GluR2 antibody (*Surface GluR2*). The overexpressed GluR2 (*Total GluR2*) or N-cadherin in each cell lysate was almost equivalent. The HNK-1 epitope was expressed on GluR2 when GlcAT-P and HNK-1ST were overexpressed. *B,* quantification of the surface expression of GluR2 in *A*. The intensity of surface GluR2 was normalized to total GluR2, and the *bar graph* shows the percentages compared with control cells ($n = 5$). *, $p < 0.05$ (two-tailed *t* test). *Error bars* indicate S.E.

and extracellular matrix proteins (tenascin-R, phosphacan, etc.) (12, 33). Thus far, most previous studies have focused on the adhesive and morphological functions of HNK-1 epitope on these molecules and have shown its relationship to neural crest cell migration, neuron to glial cell adhesion, and the outgrowth of astrocytic processes (3). From the aspect of synaptic plasticity, the HNK-1 epitope carried by tenascin-R has been well characterized. Tenascin-R is highly present in the perineuronal nets surrounding parvalbumin-positive inhibitory interneurons (34, 35). It is proposed that HNK-1 epitope on tenascin-R is involved in the regulation of perisomatic inhibition of CA1 pyramidal neurons via reduction of evoked γ-aminobutyric acid release, resulting in the reduction of LTP in CA1 pyramidal neurons (12, 36). In this study, we report that the HNK-1 epitope is expressed at excitatory postsynaptic sites on hippocampal pyramidal neurons (Fig. 1). We first identified the neurotransmitter receptor subunit GluR2 as a

novel HNK-1 carrier molecule (Figs. 2 and 3). HNK-1 regulates the synaptic functions of GluR2 by modulating the surface expression of GluR2 (Figs. 4 and 6). This study provides new aspects for understanding the role of HNK-1 glyco-epitope in synaptic plasticity.

In mature pyramidal neurons, GluR1 and GluR2 are predominantly expressed, and the great majority of AMPA receptors contain GluR2 subunits. In particular, it is considered that GluR2 subunit plays pivotal roles in receptor assembly and trafficking (15, 37). GluR1 and GluR2 are synthesized and assembled into tetrameric AMPA receptor complexes in the endoplasmic reticulum. After their assembly, the HNK-1 on GluR2 is synthesized by GlcAT-P and HNK-1ST in the Golgi apparatus. GluR2 has four *N*-glycosylation sites in its extracellular N-terminal domain, and all of them are conserved between GluR2 and GluR1 (16). Interestingly, although GluR1 and GluR2 have high homology with respect to their amino acid sequence and common biosynthesis pathway, HNK-1 is selectively expressed on GluR2 but not on GluR1. This result suggests that HNK-1 regulates the specific function of GluR2 and influences excitatory synaptic transmissions.

It has been widely demonstrated that GluR2 interacts with its intracellular and extracellular partners, and these interactions control AMPA receptor functions such as receptor trafficking and stabilization on the cell surface (38). Glutamate receptor interacting protein/AMPA-binding protein and protein interacting with protein kinase C-1 are partners that associate with the PDZ domain in the intracellular C-terminal tail of GluR2. The interactions of glutamate receptor interacting protein/AMPA-binding protein and protein interacting with protein kinase C-1 with GluR2 depend on the phosphorylation status of the C terminus of GluR2 (including Ser-880 and Tyr-876 residues) (39–41). Another intracellular partner, *N*-ethylmaleimide-sensitive fusion protein, binds to the C-terminal membrane-proximal site of GluR2 and plays important roles in the insertion of AMPA receptors into postsynaptic membranes (42, 43). This *N*-ethylmaleimide-sensitive fusion protein-binding site overlaps with the binding site of AP2, which is an adaptor protein for cargo in clathrin-dependent endocytosis (30, 44). We examined the interactions of GluR2 with these proteins, but there was no apparent difference between wild-type and GlcAT-P-deficient mice (data not shown). As for the extracellular N-terminal domain of GluR2, there are few reports about its functions and interactions with its partners. Passafaro *et al.* (45) demonstrated that the overexpression of the GluR2 N-terminal domain exhibited an increase in the number of functional synapses and enlargement of spine heads in cultured hippocampal neurons. A recent study (31) showed that the interaction with N-cadherin is needed for the synapse (spine) promotion activity and stabilization of GluR2 on the neuronal surface. In this study, the absence of the HNK-1 epitope on GluR2 reduced its interaction with N-cadherin *in vivo* and *in vitro* (Fig. 5). Corresponding to this, we observed the abnormal dendritic spine morphogenesis in early postnatal GlcAT-P-deficient mice and in cultured hippocampal neurons.[4] During

---

[4] I. Morita, S. Kakuda, Y. Takeuchi, T. Kawasaki, and S. Oka, unpublished data.

synaptogenesis (at postnatal day 14), most pyramidal neurons in wild-type mice possessed mature spines with mushroom-like heads, but the majority of dendritic protrusions were long and thin immature filopodia-like spines in GlcAT-P-deficient mice. These data led us to suggest that HNK-1 on GluR2 controls not only AMPA receptor trafficking but also spine morphogenesis. However, HNK-1 is widely expressed on a series of cell adhesion molecules and extracellular molecules other than GluR2 (Fig. 1). As the HNK-1 on these molecules has almost completely disappeared in GlcAT-P-deficient mice (Fig. 1), it is difficult to rule out the involvement of the HNK-1 on other molecules in spine morphology. Although we reveal in this study that HNK-1 on GluR2 is probably involved in synaptic plasticity by regulating its cell surface expression level through its interaction with N-cadherin *in vivo*, further investigation is necessary to clarify the precise molecular mechanisms of spine formation and synaptic plasticity regulated by the HNK-1 glyco-epitope.

REFERENCES

1. Morita, I., Kizuka, Y., Kakuda, S., and Oka, S. (2008) *J. Biochem.* **143,** 719–724
2. Künemund, V., Jungalwala, F. B., Fischer, G., Chou, D. K., Keilhauer, G., and Schachner, M. (1988) *J. Cell Biol.* **106,** 213–223
3. Bronner-Fraser, M. (1987) *Dev. Biol.* **123,** 321–331
4. Martini, R., Xin, Y., Schmitz, B., and Schachner, M. (1992) *Eur. J. Neurosci.* **4,** 628–639
5. Terayama, K., Oka, S., Seiki, T., Miki, Y., Nakamura, A., Kozutsumi, Y., Takio, K., and Kawasaki, T. (1997) *Proc. Natl. Acad. Sci. U.S.A.* **94,** 6093–6098
6. Seiki, T., Oka, S., Terayama, K., Imiya, K., and Kawasaki, T. (1999) *Biochem. Biophys. Res. Commun.* **255,** 182–187
7. Bakker, H., Friedmann, I., Oka, S., Kawasaki, T., Nifant'ev, N., Schachner, M., and Mantei, N. (1997) *J. Biol. Chem.* **272,** 29942–29946
8. Rabouille, C., Hui, N., Hunte, F., Kieckbusch, R., Berger, E. G., Warren, G., and Nilsson, T. (1995) *J. Cell Sci.* **108,** 1617–1627
9. Yamamoto, S., Oka, S., Inoue, M., Shimuta, M., Manabe, T., Takahashi, H., Miyamoto, M., Asano, M., Sakagami, J., Sudo, K., Iwakura, Y., Ono, K., and Kawasaki, T. (2002) *J. Biol. Chem.* **277,** 27227–27231
10. Strekalova, T., Wotjak, C. T., and Schachner, M. (2001) *Mol. Cell. Neurosci.* **17,** 1102–1113
11. Pradel, G., Schachner, M., and Schmidt, R. (1999) *J. Neurobiol.* **39,** 197–206
12. Saghatelyan, A. K., Gorissen, S., Albert, M., Hertlein, B., Schachner, M., and Dityatev, A. (2000) *Eur. J. Neurosci.* **12,** 3331–3342
13. Yoshihara, T., Sugihara, K., Kizuka, Y., Oka, S., and Asano, M. (2009) *J. Biol. Chem.* **284,** 12550–12561
14. Derkach, V. A., Oh, M. C., Guire, E. S., and Soderling, T. R. (2007) *Nat. Rev. Neurosci.* **8,** 101–113
15. Isaac, J. T., Ashby, M., and McBain, C. J. (2007) *Neuron* **54,** 859–871
16. Pasternack, A., Coleman, S. K., Féthière, J., Madden, D. R., LeCaer, J. P., Rossier, J., Pasternack, M., and Keinänen, K. (2003) *J. Neurochem.* **84,** 1184–1192
17. Hall, R. A., Hansen, A., Andersen, P. H., and Soderling, T. R. (1997) *J. Neurochem.* **68,** 625–630
18. Standley, S., Tocco, G., Wagle, N., and Baudry, M. (1998) *J. Neurochem.* **70,** 2434–2445
19. Everts, I., Villmann, C., and Hollmann, M. (1997) *Mol. Pharmacol.* **52,** 861–873
20. Maruo, K., Nagata, T., Yamamoto, S., Nagai, K., Yajima, Y., Maruo, S., and Nishizaki, T. (2003) *Brain Res.* **977,** 294–297
21. Sakimura, K., Bujo, H., Kushiya, E., Araki, K., Yamazaki, M., Yamazaki, M., Meguro, H., Warashina, A., Numa, S., and Mishina, M. (1990) *FEBS Lett.* **272,** 73–80
22. Kizuka, Y., Matsui, T., Takematsu, H., Kozutsumi, Y., Kawasaki, T., and Oka, S. (2006) *J. Biol. Chem.* **281,** 13644–13651
23. Uemura, K., Kihara, T., Kuzuya, A., Okawa, K., Nishimoto, T., Ninomiya, H., Sugimoto, H., Kinoshita, A., and Shimohama, S. (2006) *Neurosci. Lett.* **402,** 278–283
24. Nakamura, M., Sato, K., Fukaya, M., Araishi, K., Aiba, A., Kano, M., and Watanabe, M. (2004) *Eur. J. Neurosci.* **20,** 2929–2944
25. Kizuka, Y., Kobayashi, K., Kakuda, S., Nakajima, Y., Itoh, S., Kawasaki, N., and Oka, S. (2008) *Glycobiology* **18,** 331–338
26. Laemmli, U. K. (1970) *Nature* **227,** 680–685
27. Kikuchi, M., Hatano, N., Yokota, S., Shimozawa, N., Imanaka, T., and Taniguchi, H. (2004) *J. Biol. Chem.* **279,** 421–428
28. Küster, B., Wheeler, S. F., Hunter, A. P., Dwek, R. A., and Harvey, D. J. (1997) *Anal. Biochem.* **250,** 82–101
29. Man, H. Y., Lin, J. W., Ju, W. H., Ahmadian, G., Liu, L., Becker, L. E., Sheng, M., and Wang, Y. T. (2000) *Neuron* **25,** 649–662
30. Lee, S. H., Liu, L., Wang, Y. T., and Sheng, M. (2002) *Neuron* **36,** 661–674
31. Saglietti, L., Dequidt, C., Kamieniarz, K., Rousset, M. C., Valnegri, P., Thoumine, O., Beretta, F., Fagni, L., Choquet, D., Sala, C., Sheng, M., and Passafaro, M. (2007) *Neuron* **54,** 461–477
32. Nuriya, M., and Huganir, R. L. (2006) *J. Neurochem.* **97,** 652–661
33. Liedtke, S., Geyer, H., Wuhrer, M., Geyer, R., Frank, G., Gerardy-Schahn, R., Zähringer, U., and Schachner, M. (2001) *Glycobiology* **11,** 373–384
34. Wintergerst, E. S., Vogt Weisenhorn, D. M., Rathjen, F. G., Riederer, B. M., Lambert, S., and Celio, M. R. (1996) *Neurosci. Lett.* **209,** 173–176
35. Brückner, G., Grosche, J., Schmidt, S., Härtig, W., Margolis, R. U., Delpech, B., Seidenbecher, C. I., Czaniera, R., and Schachner, M. (2000) *J. Comp. Neurol.* **428,** 616–629
36. Dityatev, A., and Schachner, M. (2003) *Nat. Rev. Neurosci.* **4,** 456–468
37. Santos, S. D., Carvalho, A. L., Caldeira, M. V., and Duarte, C. B. (2009) *Neuroscience* **158,** 105–125
38. Bassani, S., Valnegri, P., Beretta, F., and Passafaro, M. (2009) *Neuroscience* **158,** 55–61
39. Matsuda, S., Launey, T., Mikawa, S., and Hirai, H. (2000) *EMBO J.* **19,** 2765–2774
40. Chung, H. J., Xia, J., Scannevin, R. H., Zhang, X., and Huganir, R. L. (2000) *J. Neurosci.* **20,** 7258–7267
41. Chung, H. J., Steinberg, J. P., Huganir, R. L., and Linden, D. J. (2003) *Science* **300,** 1751–1755
42. Nishimune, A., Isaac, J. T., Molnar, E., Noel, J., Nash, S. R., Tagaya, M., Collingridge, G. L., Nakanishi, S., and Henley, J. M. (1998) *Neuron* **21,** 87–97
43. Noel, J., Ralph, G. S., Pickard, L., Williams, J., Molnar, E., Uney, J. B., Collingridge, G. L., and Henley, J. M. (1999) *Neuron* **23,** 365–376
44. Kastning, K., Kukhtina, V., Kittler, J. T., Chen, G., Pechstein, A., Enders, S., Lee, S. H., Sheng, M., Yan, Z., and Haucke, V. (2007) *Proc. Natl. Acad. Sci. U.S.A.* **104,** 2991–2996
45. Passafaro, M., Nakagawa, T., Sala, C., and Sheng, M. (2003) *Nature* **424,** 677–681